

Switching between coherent and incoherent singlet fission via solvent-induced symmetry-breaking

Antonios M Alvertis, Steven Lukman, Timothy J. H. Hele, Eric G Fuemmeler, Jiaqi Feng, Jishan Wu, Neil C. Greenham, Alex W Chin, and Andrew J. Musser

J. Am. Chem. Soc., **Just Accepted Manuscript** • DOI: 10.1021/jacs.9b05561 • Publication Date (Web): 11 Oct 2019

Downloaded from pubs.acs.org on October 23, 2019

Just Accepted

“Just Accepted” manuscripts have been peer-reviewed and accepted for publication. They are posted online prior to technical editing, formatting for publication and author proofing. The American Chemical Society provides “Just Accepted” as a service to the research community to expedite the dissemination of scientific material as soon as possible after acceptance. “Just Accepted” manuscripts appear in full in PDF format accompanied by an HTML abstract. “Just Accepted” manuscripts have been fully peer reviewed, but should not be considered the official version of record. They are citable by the Digital Object Identifier (DOI®). “Just Accepted” is an optional service offered to authors. Therefore, the “Just Accepted” Web site may not include all articles that will be published in the journal. After a manuscript is technically edited and formatted, it will be removed from the “Just Accepted” Web site and published as an ASAP article. Note that technical editing may introduce minor changes to the manuscript text and/or graphics which could affect content, and all legal disclaimers and ethical guidelines that apply to the journal pertain. ACS cannot be held responsible for errors or consequences arising from the use of information contained in these “Just Accepted” manuscripts.

Switching between coherent and incoherent singlet fission via solvent-induced symmetry-breaking

Antonios M. Alvertis^{1,†}, Steven Lukman^{2,†}, Timothy J. H. Hele¹, Eric G. Fuemmeler³, Jiaqi Feng⁴, Jishan Wu⁴, Neil C. Greenham¹, Alex W. Chin⁵, Andrew J. Musser^{3,6,*}

¹Cavendish Laboratory, University of Cambridge, J. J. Thomson Avenue, Cambridge CB3 0HE, United Kingdom

²Institute of Materials Research and Engineering, Agency for Science Technology and Research (A*STAR), 2 Fusionopolis Way, Singapore 138634, Singapore.

³Department of Chemistry and Chemical Biology, Cornell University, Ithaca, NY 14853

⁴Department of Chemistry, National University of Singapore, 3 Science Drive 3, 117543, Singapore

⁵CNRS & Institut des NanoSciences de Paris, Sorbonne Université, 4 place Jussieu boîte courrier 840, 75252 Paris Cedex 05, France.

⁶Department of Physics and Astronomy, University of Sheffield, Hounsfield Road, Sheffield S3 7RH, UK.

[†]These authors contributed equally.

*e-mail: ajm557@cornell.edu

Abstract

Singlet fission in organic semiconductors causes a singlet exciton to decay into a pair of triplet excitons and holds potential for increasing the efficiency of photovoltaic devices. In this combined experimental and theoretical study, we reveal that a covalent dimer of the organic semiconductor tetracene undergoes activated singlet fission by qualitatively different mechanisms depending on the solvent environment. We show that intramolecular vibrations are an integral part of this mechanism, giving rise to mixing between charge transfer and triplet pair excitations. Both coherent or incoherent singlet fission can occur, depending on transient solvent-induced energetic proximity between the states, giving rise to complex variation of the singlet fission mechanism and timescale in the different environments. Our results suggest a more general principle for controlling the efficiency of photochemical reactions by utilizing transient interactions to tune the energetics of reactant and product states and switch between incoherent and coherent dynamics.

Introduction

Singlet fission¹ is an electronic process in organic materials which has been extensively studied in the past decade. This is largely because of its promise for efficient solar energy technologies which surpass the Shockley-Queisser limit.² Singlet fission converts a high-energy singlet exciton to two low-energy triplet excitons, which are at least initially coupled into an overall singlet state. Thus singlet fission conserves spin, allowing it to be an ultra-fast process and effectively compete with radiative and non-radiative deactivation of excited states. This energetic down-conversion process offers a way to overcome thermalization losses, and has inspired the design of new hybrid device concepts.^{3,4} However, the primary interest in the field to date remains building a more detailed understanding of the underlying photophysical mechanism, with the aim of informing rational materials design.

There have been multiple reports that singlet fission can occur through an ultrafast (fs-ps) ‘coherent’ mechanism.⁵⁻⁹ Here, photoexcitation is thought to generate an initial superposition of the lowest bright singlet state S_1 and the dark double-triplet state TT which eventually dephases into the dark state. In some materials, this coherent regime is reported to coexist with slower, incoherent fission dynamics,^{8,9} in which S_1 ‘hops’ to the TT surface non-adiabatically, or adiabatically relaxes into the TT region on the same potential energy surface. Incoherent singlet fission is the more commonly invoked picture, particularly when it occurs on longer ($>$ ps) timescales.^{10,11} Interestingly, even in systems where it is endothermic, e.g. in tetracene,¹²⁻¹⁵ singlet fission can be very efficient and temperature-independent.¹⁴⁻¹⁷ To explain such observations, coherent processes have been invoked.^{9,18}

Despite recent progress in understanding the coherent mechanism of singlet fission and its interplay with incoherent dynamics, what has thus far been missing is a tuneable way of switching between the two regimes. This is partly because there are no established experimental handles to achieve this, and the utility of coherent dynamics as a concept for materials design and eventual applications is not clear. Similarly to many other photophysical processes in organic molecules, one of the most promising angles to explore coherent dynamics is through molecular vibrations. These are increasingly recognized both in experiment^{9,16,19,20} and theory²¹⁻²⁶ to play a critical role in the ultra-fast regime where singlet fission is often found to occur. The coherent mechanism of singlet fission in rubrene (which has a well-defined symmetry) has been shown to arise via symmetry-breaking modes that allow S_1 and TT to mix.⁹ More broadly, when the mixing between electronic states in such systems is governed by coupling to intramolecular motions, to some extent it can be tuned, for example by controlling the viscosity of the environment²⁷ or chemically introducing steric barriers.²⁸ This control is rather limited and poorly understood, especially in solid-state systems where the complex interplay of intra- and intermolecular vibrations must be considered.

Another critical ingredient in both coherent and incoherent fission mechanisms that has proved most difficult to explore is the nature of the coupling that results in quantum superpositions or population transfer between S_1 and TT. There has been extensive debate about the relative strength and influence of ‘direct’ two-electron coupling between these states, versus sequential one-electron couplings mediated by a charge-transfer (CT)

1
2
3 state.^{1,11,29–32} Couplings involving the CT state are typically expected to be orders of magnitude higher, but
4 in conventional thin-film systems there is no experimental means to perturb the CT manifold, especially if the
5 states are not directly populated but only mediate fission through super-exchange as ‘virtual’ intermediates.^{29,32}
6 However, covalent dimers of singlet-fission chromophores offer exquisite tunability of the critical interactions that
7 govern fission, both through chemical design^{33–43} and the external environment,^{27,44,45} and they thus present
8 the most promising platform to describe and control such effects. In these systems, the energies of CT states can
9 be directly tuned through the use of different solvents. This concept has enabled the demonstration of fission
10 mediated by direct S₁-TT coupling,²⁸ virtual CT states^{26,27,44,45} and even a distinct CT intermediate.²⁷ In
11 short, covalent dimers offer a versatile platform to systematically explore the S₁-TT transition and understand
12 the nature of the coherent/incoherent pathways.

13
14 Here, we employ a combination of ultrafast spectroscopy and theoretical techniques to reveal the detailed
15 mechanism of singlet fission in the orthogonal tetracene dimer DT-Mes (Figure 1a) in solution and demonstrate
16 how it is governed by a tuneable ‘switch’ between the incoherent and coherent regimes. Our experimental
17 findings show that singlet fission in this system is a ‘hot’ process, i.e. it only occurs upon excitation distinctly
18 above the band-edge of the first excited singlet state.⁴⁶ Its mechanism is found to be qualitatively different
19 depending on the solvent environment, and the fission efficiency is maximized in intermediate polarity solvents.
20 Our theoretical analysis allows us to identify the crucial role of molecular vibrations to the singlet fission
21 process, though alone they only give rise to weak mixing between states participating in singlet fission, and can
22 only account for the experimental observations in low-polarity solvents where the process is incoherent. In more
23 polar solvents we observe a qualitatively different regime of singlet fission, and we can only capture this behavior
24 through the inclusion of dynamic solvent effects. Our model reveals that increasing the polarity switches DT-Mes
25 into a regime of coherent singlet fission. However, contrary to previous studies reporting on superpositions of
26 S₁ and TT that dephase into the triplet pair,^{6,7,9,18} here we show that the coherent mechanism comes into play
27 through the mixing of a CT state and TT. Coherent singlet fission occurs in solvents of intermediate polarity,
28 where dynamic solvent effects induce the closest energetic proximity between these states so that molecular
29 vibrations can mix them most efficiently. It is precisely the properties of CT states which allow us to tune them
30 through the dielectric environment, which in contrast to local-excitations and triplet pairs, have a finite electric
31 dipole. This underlines the novelty of our ‘switch’ mechanism, and emphasizes the potential of using CT states
32 to tune coherent dynamics.

33 34 35 36 37 38 39 40 41 42 43 44 45 46 47 48 **Results and discussion**

49
50 **Molecular structure and coupling.** DT-Mes (chemical structure in Figure 1a) consists of two tetracenes
51 directly linked at the 5,5’ position, with mesityl side groups for solubility. The synthesis and purification are
52 described in SI section S2.1. Similarly to the anthracene⁴⁷ and pentacene²⁷ analogs and a closely related cyano-
53 substituted tetracene dimer,⁴⁸ DFT geometry optimization reveals that steric repulsion forces the two tetracenes
54 into an orthogonal geometry. Being an alternate hydrocarbon, DT-Mes has no permanent dipole in the ground
55
56
57
58
59
60

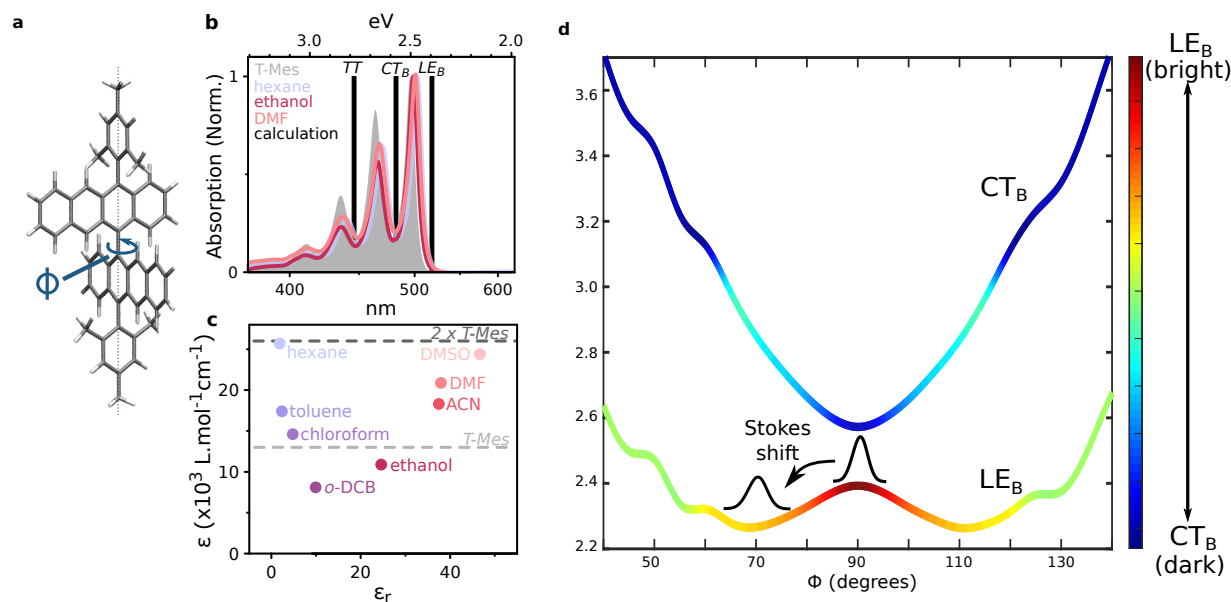


Figure 1 | DT-Mes structure and photophysics. (a) Chemical structure of DT-Mes in its orthogonal ground-state geometry, indicating the dominant torsional motion. (b) Ground state absorption spectra of DT-Mes in solvents of different polarity and mesityl-substituted tetracene monomer T-Mes in chloroform (shaded). Calculated electronic energy levels are shown as vertical bars. The energy of the bright state LE_B is in excellent agreement with the position of the absorption onset. (c) Peak molar extinction coefficient of DT-Mes in different solvents compared to that of T-Mes in chloroform (dashed). The extinction coefficient is minimized in intermediate polarity solvents. (d) Potential energy surfaces of the two bright excited states along the torsional coordinate. The color code indicates the mixing between the LE_B and CT_B surfaces, leading to finite oscillator strength for the latter through intensity borrowing. The maximal mixing is found at the local minima of LE_B , from where strongly red-shifted emission occurs.

electronic state, as predicted from the Coulson-Rushbrooke theorem.⁴⁹ Therefore, the ground state geometry does not depend on the dielectric environment.

The orthogonal geometry raises the question of whether the two tetracenes can interact electronically, given their negligible π overlap.^{27,44} We determine the presence and relative strength of interchromophore coupling from the steady-state absorption (Figure 1b). This does not directly map onto the excited-state couplings between dark states (CT and TT) actually relevant to singlet fission,³⁸ but it serves as a useful proxy.¹⁰ Compared to the equivalent mesityl-tetracene monomer (shaded), the dimer (lines) exhibits a more prominent 0-0 absorption peak, though the exact 0-0/0-1 ratio varies with solvent. The enhanced 0-0 peak reflects J-type excitonic coupling between the short-axis-polarized $S_0 \rightarrow S_1$ transitions of the tetracenes. Moreover, the solvent dielectric constant has a powerful effect on the molar extinction coefficient (Figure 1c). In the extremes of our solvent polarity series we find that the dimer absorbs two times as strongly as the monomer. This would be consistent with negligible inter-tetracene interactions, similar to several prior reports of weakly coupled dimers.³⁴⁻³⁷ However, in intermediate solvents the extinction coefficient of the dimer is less than that of even a single monomer, reaching as low as 40% of the expected value. This strong hypochromism is compelling evidence for strong interchromophore coupling, presumably mediated by interaction with dark charge-transfer (CT) states²⁷ given the strong solvent dependence. This is further supported by the model approach which is developed in this work (see below), which reproduces the behavior of the molar extinction coefficient in different solvents due to mixing with the CT states (SI Section S1.3). As in the equivalent pentacene dimers,^{27,44} we

propose that the tetracenes are simultaneously coupled through CT and excitonic interactions. These have opposite effects on the energy of the bright state (a red-shift from the excitonic coupling and a blue-shift from the CT-mediated coupling), and the combination results in ‘null aggregates’ with weak spectral shifts and small changes in vibronic structure despite the significant interactions.⁵⁰ Within this framework, the results in Figure 1c demonstrate that CT states play a central and tuneable role in the dimer electronic structure.

Exciton states and state mixing. In describing the electronic structure and properties of DT-Mes, we use as our basis the five lowest-energy adiabatic excited states in the orthogonal ground-state geometry, calculated in the absence of solvent effects. For a detailed definition of the electronic basis and full computational details please refer to SI Section S1.1. The molecule has approximate C_2 symmetry, thus the excited singlets transform either as the totally symmetric irreducible representation A or the antisymmetric B . The two lowest-energy adiabatic singlets are the localized excitations LE_B and LE_A , while the next two are the close-to-degenerate charge-transfer CT_A and CT_B states. The LE states refer to intra-monomer transitions, while CT states include a transition which is delocalized over both tetracene monomers. Among these states, only LE_B is bright at the Franck-Condon (FC) point. Its calculated energy (vertical bar in Figure 1b) is in excellent agreement with our experimental measurements. Likewise, the predicted energies of CT_B agree to within ≈ 0.1 eV with the experimentally determined vacuum CT level. Apart from these single excitations, we approximate the triplet pair state resulting from singlet fission as the ground state quintet 5TT (SI Section S1.1) of DT-Mes.

The above states constitute our electronic basis, however once semi-classical vibrational and/or solvent effects are taken into account (see below), a typical adiabatic excited state $|\Psi\rangle$, will, in general, become a superposition of these basis states:

$$|\Psi\rangle = c_{LE_B} |LE_B\rangle + c_{LE_A} |LE_A\rangle + c_{CT_A} |CT_A\rangle + c_{CT_B} |CT_B\rangle + c_{TT} |TT\rangle \quad (1)$$

To make it easier to compare spectroscopic and theoretical results, we label these superposition states according to their dominant contribution, e.g. if $|LE_B\rangle$ dominates the sum of Equation 1, we call the state LE_B for simplicity. We stress that this convention is not meant to imply that the state $|\Psi\rangle$ is exactly equal to one of the basis states, which are only present in their pure form in the ground-state geometry at low polarity. For such a superposition state $|\Psi\rangle$, the mixing between two of its basis states, e.g. CT_B and TT , is defined as:

$$\rho_{CT_B TT} = c_{CT_B}^* \cdot c_{TT}. \quad (2)$$

It is obvious that this mixing will strongly depend on the choice of electronic basis, and it is always possible to work in a basis where it vanishes. Here we work in the basis of the diabatic states shown in Equation 1, which are themselves equal to the *adiabatic* states at the FC point and in a non-polar solvent. Therefore, initial photoexcitation forms a pure LE_B state, and any subsequent mixing occurs between states that were originally separate, and is not an artifact of our choice of basis.

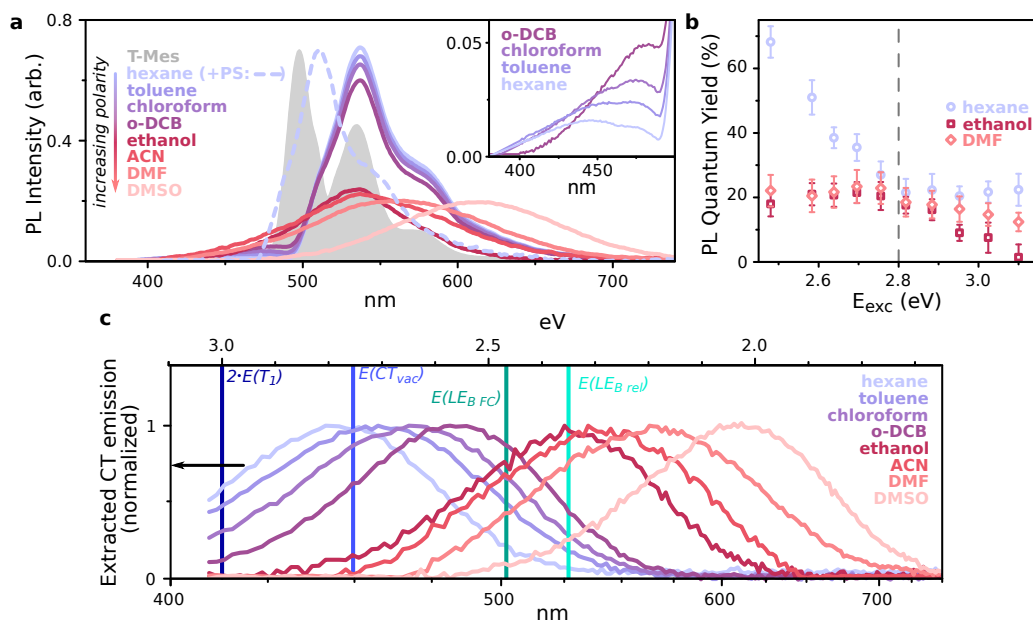


Figure 2 | Multiple emissive species (a) Steady-state photoluminescence of DT-Mes in a range of solvents (solid lines), following excitation at 3.1 eV. The red-shift relative to monomer T-Mes (grey shaded) can be suppressed in high-viscosity solution (dashed). Inset: non-Kasha emission observed in non-polar solvents. (b) Solvent- and excitation-dependent photoluminescence quantum yield. In all media, the behavior of the system changes markedly for excitation at energies above 2.8 eV. (c) Energy landscape constructed from emission measurements. CT_{\downarrow} spectra (lines) are extracted from time-resolved emission measurements in each solvent (SI Figs. S27, S28). Vertical bars denote the energies of other relevant electronic states. LE_{BFC} and LE_{Brel} are determined in non-polar solvents with and without polystyrene. $E(T_1)$ is determined from sensitized phosphorescence (SI Fig. S9) and $E(CT_{vac})$ is extrapolated from the CT solvent dependence (see Figure 5 below). The energies of all emissive states are below the presumed singlet fission threshold $2 \cdot E(T_1)$.

To investigate the effect of molecular vibrations on the photophysics, we perform electronic structure calculations for a range of displacements along the torsional angle Φ between the monomers (Figure 1a). This motion crucially underpins the photophysics of both the anthracene⁴⁷ and pentacene²⁷ analogs. In DT-Mes, this is a low-frequency motion (39.6 cm^{-1}) of A symmetry. From analyzing the excitation character of the surfaces, we conclude that displacement along Φ leads to mixing between bright LE_B and dark CT_B (Figure 1d). This results in CT_B borrowing intensity from LE_B and becoming partially bright.⁵¹ Our calculations also reveal energetic relaxation of LE_B with increasing Φ and away from the FC point, to a minimum at 70° . This tendency towards planarization gives rise to Stokes-shifted emission (see below) and is also documented in the equivalent anthracene⁴⁷ and pentacene²⁷ dimers.

In a final clarification about notation, we point out that solvent effects result in mixing between the two symmetry-pure CT states. This results in the formation of two new CT states which are linear combinations of the originals. One of these has lower energy, which we denote as CT_{\downarrow} , while the other one is destabilized and denoted as CT_{\uparrow} . Both of these have finite CT_B character, hence both borrow intensity from LE_B and are partially bright, with the potential to emit photons. However, in practice we only detect photon emission from CT_{\downarrow} . For ease we use this as the primary label for CT-related experimental signatures, with the recognition that it denotes a solvent-dependent mixture of CT_B and CT_A . We discuss the nature and implications of this mixing in greater detail below, following the presentation of experimental data.

Multiple emissive species. We define the energetic landscape of DT-Mes through photoluminescence

1
2 spectroscopy. Though the steady-state absorption spectra of monomer and dimer are almost identical (Figure
3 1a), the steady-state photoluminescence of DT-Mes in solution (Figure 2a, solid lines) exhibits a large Stokes
4 shift of ≈ 35 nm not observed in the monomer (shaded spectrum, ≈ 2 nm). This shift can be reduced in
5 high-viscosity polystyrene solution (dashed spectrum), confirming that it is linked to large-scale conformational
6 change such as relaxation along Φ . These measurements also show a more pronounced solvent dependence than
7 the steady-state absorption. In the four least-polar solvents the emission is dominated by a well-defined vibronic
8 progression (500 nm–600 nm) which does not shift and can be assigned to the relaxed (i.e. partially planarized)
9 singlet LE_{Brel} . In the more polar solvents, the emission becomes featureless and progressively red-shifts with
10 increasing polarity. This behavior is a hallmark of CT state emission.^{27,52} Similar features are also detected
11 at the high-energy edge in non-polar solvents (inset), i.e. at shorter wavelengths than LE_B photoluminescence.
12 This non-Kasha emission, from a state which is not the lowest-energy singlet in the molecule, is surprising,
13 though long-lived high-energy CT states are known in similar orthogonal systems.⁵³ Here, it indicates the
14 presence of multiple emissive species (LE_B and CT_{\downarrow}) in DT-Mes in non-polar solvents.

15
16 In non-polar solvents, it is possible to tune the balance of these species through the pump photon energy
17 (full characterization in SI Section S2.9). Band-edge excitation in hexane yields purely excitonic emission, with
18 a quantum efficiency of $\approx 68\%$ (Figure 2b). With increasing photon energy, we detect a greater proportion of
19 non-Kasha CT_{\downarrow} emission, as shown in the photoluminescence excitation maps in SI Figure S28. This changing
20 balance is accompanied by a corresponding decrease in the photoluminescence quantum yield until saturation
21 at $\approx 20\%$. This is comparable to the quantum yield when the emission is dominated by CT_{\downarrow} , as observed in
22 all polar solvents following band-edge excitation. Interestingly, the behavior of the emission quantum efficiency
23 qualitatively changes for excitation above the pump photon energy threshold of 2.8 eV both for polar and non-
24 polar solvents - monotonic decrease and saturation, respectively. This behavior suggests a significant change in
25 photophysical processes above this energy.

26
27 To guide our analysis of these excitation-dependent processes, we first compile the essential results from
28 photoluminescence measurements to describe the DT-Mes energetic structure. Time-correlated single-photon
29 counting (SI Section S2.9) reveals that in non-polar solvents the non-Kasha CT_{\downarrow} emission has a lifetime of \approx
30 20 ns. This is comparable to what we observe in polar solvents, where CT_{\downarrow} is the only emissive species. This
31 is significantly longer than the excitonic LE_B emission observed in polar solvents, which has a lifetime of \approx
32 6 ns. This large difference allows straightforward spectral decomposition to isolate the CT_{\downarrow} emission spectra,
33 plotted for all solvents in Figure 2c. We compare this emission to the energies of key electronic states (vertical
34 bars). Unsurprisingly, examination of the CT_{\downarrow} and excitonic energies reveals that CT emission dominates in
35 the four polar solvents in which CT_{\downarrow} is the lowest-energy state. Comparing to Figure 1c, we also find that
36 the minimum in extinction coefficient coincides with the point at which $E(CT_{\downarrow})$ is closest to $E(LE_{BFC})$. This
37 energetic proximity presumably enables the strongest CT-mediated coupling between tetracenes. Interestingly,
38 sensitized phosphorescence measurements show that the dimerization motif of DT-Mes substantially destabilizes
39 the triplet state from 1.3 eV to 1.5 eV (SI Figure S9), which is denoted by the vertical bar at 3 eV. This is a
40 surprising effect which was also observed in orthogonal pentacene dimers,²⁷ and its origin is not currently
41
42
43
44
45
46
47
48
49
50
51
52
53
54
55
56
57
58
59
60

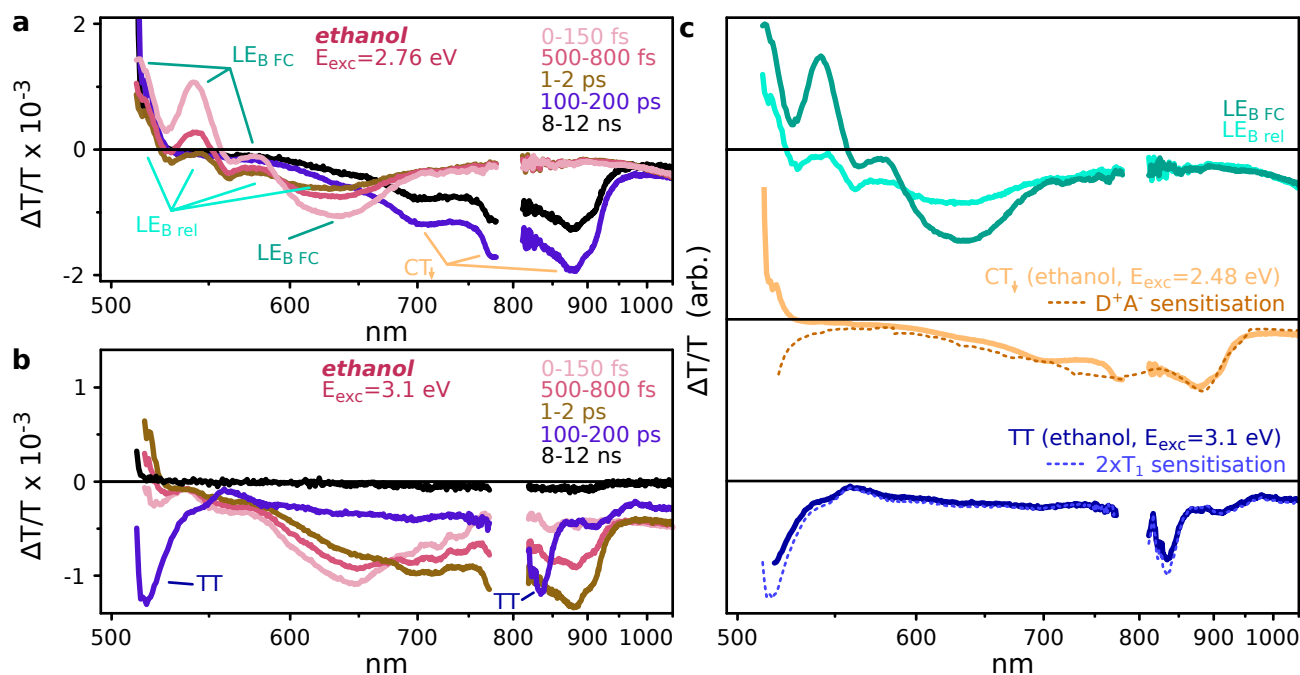


Figure 3 | Excited-state evolution in DT-Mes. (a) Transient absorption spectra of DT-Mes in ethanol for excitation below the 2.8 eV threshold. Signatures of LE_{BFC} , LE_{Brel} and CT_{\downarrow} are indicated. (b) $E_{exc} > 2.8$ eV generates a different initial state from lower-energy excitation. This state evolves into the same CT_{\downarrow} signatures (1 ps–2 ps) observed in a. Subsequent CT_{\downarrow} decay yields distinctive TT signatures (indicated), which largely decay < 1 ns. (c) Species-associated spectra extracted from transient absorption spectroscopy (solid) and reference spectra from charge and triplet sensitization (dashed). The relative magnitudes of the spectra reflect their relative molar extinction coefficients. See SI Section 2.11 for details.

understood. We recall, though, that previous studies on perylene diimide films found the triplet energy varies with intermolecular coupling,⁵⁴ and significant energy shifts have been reported between TIPS-tetracene⁵⁵ and a phenyl-substituted derivative.⁵⁶ There is evidently significant scope - currently little explored - to tune the triplet energy on the same parent chromophore. The crucial result of these measurements for our purposes here is that none of the states observed in absorption or emission approach the energy expected to be required for singlet fission. Nor is it immediately evident what is the origin of the observed thresholding behavior appearing at 2.8 eV in Figure 2b, since it would not be expected to arise from singlet fission.

CT-mediated singlet fission. To better understand the system's behavior and the role of dark electronic states, we have probed the dynamics of DT-Mes using transient absorption spectroscopy in all eight solvents with ten pump photon energies, spanning from band-edge excitation (2.48 eV) to significant excess energy (3.10 eV). We present representative results for ethanol solution in Figure 3, with detailed spectra and kinetics available in SI Section S2.6. Below the 2.8 eV excitation threshold (Figure 3a) we can identify the signatures of three distinct electronic states. The initial state LE_{BFC} is characterized by a prominent trio of stimulated emission ($\Delta T/T > 0$) peaks at 510 nm, 540 nm and 580 nm and a well-defined excited-state absorption ($\Delta T/T < 0$) at 630 nm. These signatures evolve with ≈ 550 fs time-constant to a state with strongly attenuated stimulated emission and a broader, flattened excited-state absorption. In corresponding transient grating photoluminescence⁵⁷ measurements (SI Section S2.8), we observe on precisely the same timescale a pronounced redshift of the emission consistent with geometric relaxation of the excited state. This 550 fs time constant is intermediate between the

1
2
3 planarization dynamics reported for the equivalent anthracene⁵⁸ and pentacene²⁷ dimers. We can thus assign
4 the second species in transient absorption to the partially planarized singlet $LE_{B_{rel}}$. On longer timescales a
5 new species is evident with unique excited-state absorption in the near-infrared (e.g. 710 nm, 775 nm, 880 nm).
6 This state is similarly long-lived to the CT_{\downarrow} emission (≈ 20 ns) and the features in the near-infrared closely
7 match peaks observed in the chemical oxidation and reduction spectra (Figure 3c and SI Section S2.11), allowing
8 assignment to the CT state. While it contains multiple radical anion and cation signature peaks, the imperfect
9 match in Figure 3c also shows that CT is not a pure D^+A^- state. We attribute the deviations from the D^+A^-
10 spectrum to LE contributions to the total wavefunction, which also give the state the ability to emit. In short,
11 we observe a simple excited-state progression from the initial bright singlet state $LE_{B_{FC}}$ to a conformationally
12 relaxed singlet $LE_{B_{rel}}$, and from there to a long-lived emissive CT state. Similar dynamics are observed in all
13 solvents, for excitation below 2.8 eV but above the energy of the CT_{\downarrow} state (which varies by solvent). We do
14 not detect any signatures of triplet excitons (Figure 3c, bottom) in these conditions, demonstrating that singlet
15 fission is inactive and intersystem crossing from LE and CT states is inefficient.

16
17 For excitation above the 2.8 eV threshold, Figure 3b, the initial excited-state absorption signature is dis-
18 torted from that of $LE_{B_{FC}}$, exhibiting much weaker stimulated emission. Nonetheless, it rapidly evolves to
19 the same CT state identified in Figure 3a. The latter now undergoes a new decay pathway. At 100 ps–200 ps
20 we detect the unique excited-state absorption fingerprint of DT-Mes triplets at 520 nm and 830 nm, identified
21 from solution sensitization (Figure 3c and SI Section S2.10). The lifetime of these triplets is ≈ 800 ps, 5000
22 times shorter than the lifetime of individual triplets in sensitization (SI Fig. S26). We are only able to explain
23 such a significant reduction in the triplet lifetime through triplet-triplet annihilation. At the low concentrations
24 and excitation densities used in our experiments, that requires two triplet excitons to be produced on a single
25 DT-Mes molecule, ruling out intersystem crossing from LE states⁵⁹ or triplet generation from CT recombi-
26 nation⁶⁰ as possible formation mechanisms. Instead, we consider this rapid annihilation of triplet pairs to be a
27 hallmark of intramolecular singlet fission, as previously observed in numerous dimer and conjugated-polymer
28 studies.^{27, 34, 45, 61–63} In the case of DT-Mes, the fission process is mediated by a CT state which is directly
29 populated and presents distinct spectroscopic features. Though often predicted,^{1, 31} this fission mechanism has
30 proven experimentally elusive and has only been conclusively identified in one other system, a similar orthogo-
31 nal pentacene dimer with TIPS solubilizing groups.²⁷ It is far more common for CT states to modulate singlet
32 fission through a ‘virtual’ or superexchange pathway,^{26, 27, 29, 44, 45} but the directly observable CT intermediate
33 here allows us to obtain deeper mechanistic insight.

34
35 **Singlet fission yield variation.** We find that the basis spectra identified in Figure 3c are sufficient to
36 describe the excited-state progression in all solvents and at all pump photon energies, enabling easy comparison
37 between experimental conditions. We highlight in Figure 4 how the terminal state branches between fission-
38 generated TT and long-lived CT at 100 ps–200 ps. At this time delay singlet fission – when it occurs – is
39 complete. In panel a we observe that the TT yield is clearly optimized for intermediate solvents such as ethanol
40 and *o*-DCB. These are the solvents where the CT and LE_B energies most closely approach (Figure 2c) and where
41 we infer the strongest LE-CT coupling from the low oscillator strength (Figure 1c). For solvents with higher or
42
43
44
45
46
47
48
49
50
51
52
53
54
55
56
57
58
59
60

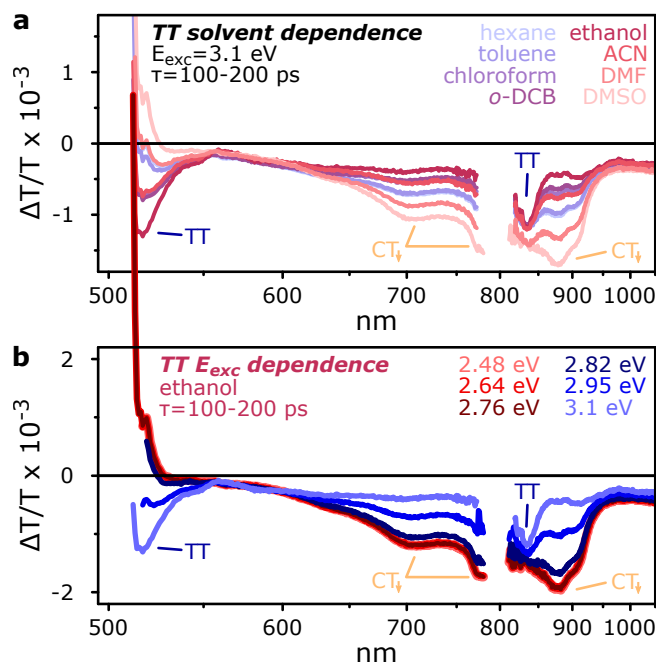


Figure 4 | Tuning the TT-CT balance. (a) Solvent dependence of TT yield at 100 ps–200 ps, following excitation at 3.1 eV. The TT yield changes depending on the dielectric environment, and is maximized in intermediate polarity solvents. (b) Pump photon energy dependence of TT yield at 100 ps–200 ps in ethanol. TT forms for excitation above 2.8 eV, and its yield increases with excitation energy up to 3.1 eV. The primary features of TT and CT_{\downarrow} are indicated again for clarity.

lower polarity, we detect increased branching into the long-lived CT_{\downarrow} state. Moreover, in ethanol the branching into TT increases monotonically with pump photon energy up to a maximum of 3.1 eV (panel b, instrument limit). The TT yield is thus a complex function of both excitation energy and solvent. The optically activated singlet fission reported in Figure 4b is particularly unusual. It has never before been observed in covalent dimers, and while it recalls the behavior of certain conjugated polymers,^{46, 63, 64} the important distinction is that the activated process is not fast. Indeed, in some of the solvents singlet fission proceeds over tens of ps, a remarkably long timescale for ‘hot’ dynamics, which we discuss further below.

Using the excited-state signatures identified in Figure 3c, we can determine the yields of TT and long-lived CT obtained in all of our transient absorption datasets. These are presented in the action spectra in Figure 5a, which summarize the full solvent- and excitation-dependent behaviors highlighted in Figure 4. The orange-shaded spectra reproduce the CT emission from Figure 2c. In polar solvents where $E(CT_{\downarrow}) < E(LE_{BFC})$ (right), the CT action spectra (circles) reveal that initial conversion into CT is always quantitative. In the non-polar solvents (left), the threshold for CT formation roughly follows the envelope of CT_{\downarrow} emission, suggesting that this emission lineshape is a reasonable proxy for the electronic energy of the state. This result demonstrates that if the initial excitation has greater energy than some portion of the broader CT_{\downarrow} distribution, then the system will access that state. We note that in non-polar solvents the total yields do not sum to 100%. In these solvents the initial formation of CT_{\downarrow} competes with relaxation into LE_{Brel} , which we can detect in transient absorption (SI Figure S36) and the vibronically structured emission (Figure 2a). This state exhibits a lifetime of ≈ 6 ns and evidently does not undergo singlet fission (SI Figure S30). The yield of LE_{Brel} is equivalent to the difference between the presented yields and 100%.

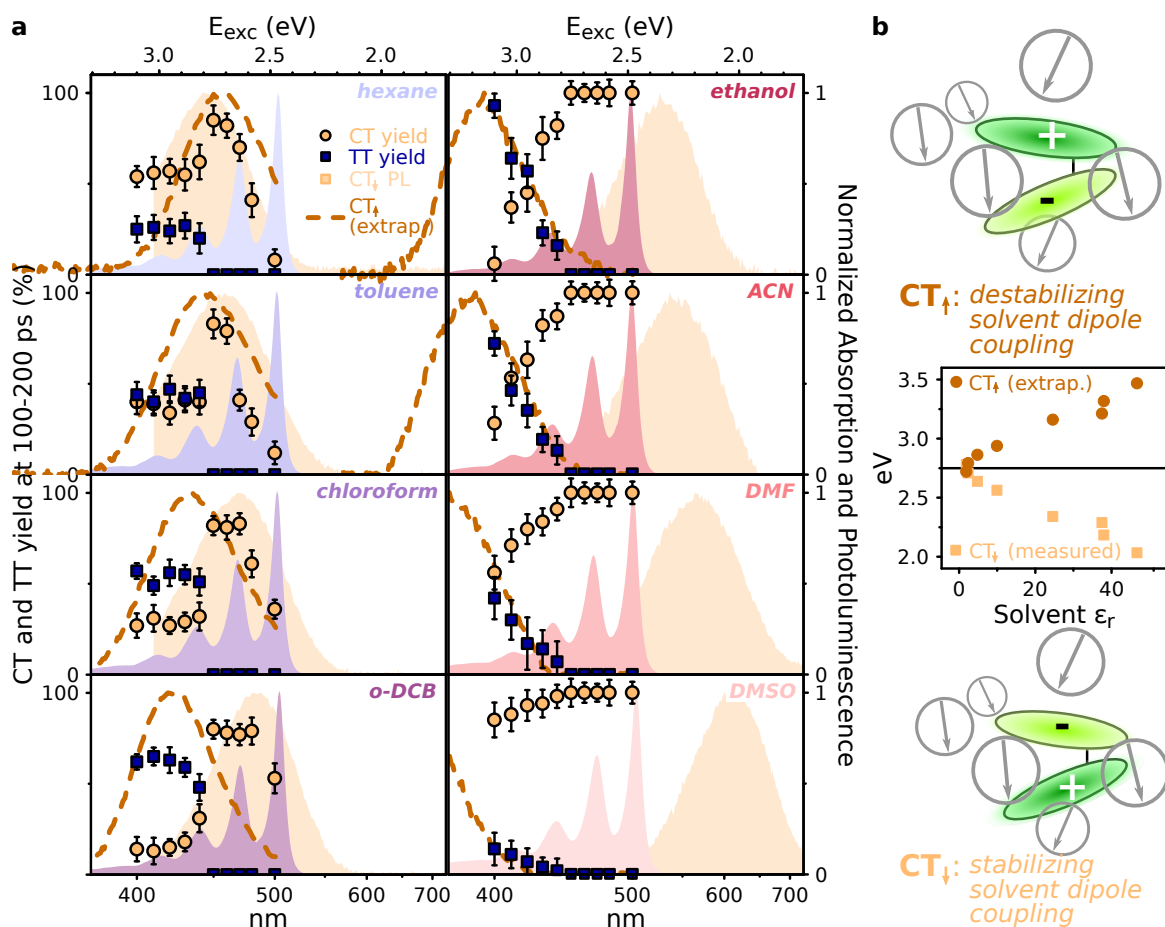


Figure 5 | TT and CT action spectra. (a) Yield of long-lived CT_↓ (circles) and TT pairs (squares), extracted from excitation-dependent transient absorption measurements at 100 ps–200 ps time delay, for solvents of increasing polarity (left to right). The TT cross-section was determined by triplet sensitization, assuming $TT \approx 2 \cdot T_1$. The CT_↓ yield is relative to the yield in ethanol following band-edge excitation, which we assume to be 100%. See SI Section S2.11 for details. Shaded spectra are steady-state absorption and extracted CT_↓ emission from Figure 2c. Dashed spectra approximate the CT_↑ distribution, by reflecting the CT_↓ emission spectrum across the vacuum CT energy CT_{vac} (see main text and panel b). (b) Peak of CT emission (squares) as a function of solvent ϵ_r allows extrapolation of the vacuum CT energy ≈ 2.75 eV (blue). CT_↓ is stabilized from this level by interactions with the solvent shell (bottom), and the oppositely polarized state would be equally destabilized (top), giving rise to the CT_↑ state (circles).

In every solvent, regardless of the threshold energy for CT formation, we observe the same threshold energy for singlet fission of ≈ 2.8 eV. It is noteworthy that this energy is significantly lower than the expected fission threshold of $2 \cdot E(T_1) \approx 3.0$ eV. It is common to invoke an entropic driving force to explain such endothermic fission in solid-state systems,^{16, 18, 65} but that should not be a factor in a strictly dimeric system. Instead, we can only rationalize this low onset energy through a binding energy. Our results imply that the immediate product of singlet fission is a bound triplet-pair state.^{16, 66–68} The spin-singlet triplet pair can be significantly stabilized relative to two ‘free’ triplets due to mixing of the diabatic TT wavefunction with other LE and CT configurations.^{24, 68, 69} While the same bound TT state is formed in all cases, the nature of the threshold appears to change from non-polar (Figure 5, left) to polar (Figure 5, right) solvents. In non-polar solvents the TT yield is nearly constant above the threshold. In polar solvents, the TT yield shows a distinctly gradual onset. We can explain this phenomenon using the pair of CT states illustrated schematically in Figure 5b. Here we recall that

the emissive CT state is stabilized by interactions with the solvation shell (bottom), hence it red-shifts as the solvent dielectric constant increases. From the solvent dependence of the CT emission we can then extrapolate the vacuum CT energy as 2.75 eV: this corresponds to the bare electronic energy of the CT state. We propose that for a given solvation shell there exists an oppositely polarized CT state (top) which will be destabilized by the same degree, though that state is not necessarily populated. To approximate the energy distribution of this CT_{\uparrow} state, we simply reflect the CT emission spectrum about the CT_{vac} level. This process generates the CT_{\uparrow} spectrum we plot in dashed lines in Figure 5a. Surprisingly, this graphical approach provides a remarkably good fit to the activation data. Our results suggest that singlet fission in polar solvents is mediated specifically by a destabilized ‘upper’ CT state, which to our knowledge has never before been observed or even suggested. To understand this behavior and the possible role such a destabilized CT state could play, we return to our theoretical description of DT-Mes.

Modelling of vibrational and solvent effects. The experimental results of the previous sections show that vibrations must be considered to explain the excited state photophysics of DT-Mes: the first step observed in transient absorption measurements is relaxation along Φ (Figure 3), and suppressing this channel through the use of polystyrene has a significant effect on the emission properties (Figure 2a). Furthermore, as summarized in Figure 5, there is a qualitative difference in the singlet fission mechanism in non-polar versus intermediate- and highly-polar solvents, while the final triplet yield also depends strongly on the excitation energy. These properties are all uncommon among singlet fission systems. It is therefore important to incorporate vibrational and solvent effects into our model description of DT-Mes, as well as the role of excess energy. We lay out here the principles of our approach; full details of the model Hamiltonian are given in SI Section S1.2.

The approximate C_2 symmetry of DT-Mes places important constraints on the fission mechanism. The TT state, which we calculate as the ground state quintet 5TT (SI Section S1.1), is A -symmetric. So is the Φ rotation of Figure 1a, meaning it only mixes states of the same symmetry. Therefore, neglecting two-electron contributions,^{1,29,31} TT only mixes with CT_A along this coordinate. However, only the bright B -symmetry states LE_B and CT_B are optically accessible. The transition from these states to TT must thus be accomplished through some form of symmetry breaking. Physically, such symmetry breaking could be provided by the vibronic coupling along a B -symmetric mode. We take $\eta = 20$ meV as a representative maximum value for this vibronic coupling, similar to values obtained for inter-molecular symmetry-breaking modes in rubrene.⁹ We introduce η in our model as the coupling of A - and B -symmetry states to each other. Therefore, a model Hamiltonian which includes the effect of the torsion and symmetry-breaking mode on the electronic states, in the basis of $\{LE_B, LE_A, CT_B, CT_A, TT\}$ is:

$$H_{el} = \begin{bmatrix} E_{LE_B}(\phi) & \eta & J(\phi) & 0 & 0 \\ \eta & E_{LE_A}(\phi) & 0 & 0 & 0 \\ J(\phi) & 0 & E_{CT_B}(\phi) & \eta & 0 \\ 0 & 0 & \eta & E_{CT_A}(\phi) & \Lambda(\phi) \\ 0 & 0 & 0 & \Lambda(\phi) & E_{TT}(\phi) \end{bmatrix}. \quad (3)$$

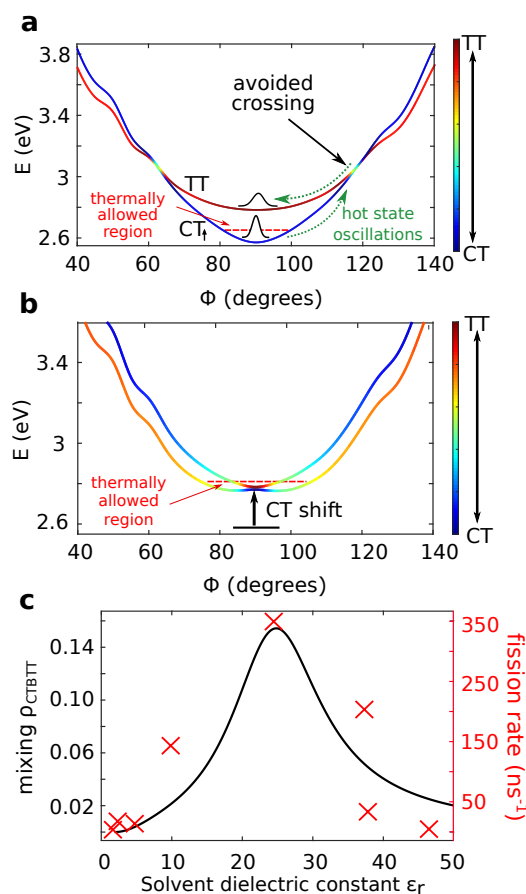


Figure 6 | Coherent and incoherent singlet fission. (a) Potential energy surfaces in non-polar solvents (e.g. hexane). CT_{\uparrow} does not mix with TT (color scale) in the thermally allowed region at room temperature, the boundaries of which are indicated with the red dashed line. Incoherent singlet fission takes place when enough excess energy to reach the avoided crossing to the TT surface is provided. (b) Potential energy surfaces for intermediate-polarity solvents (e.g. ethanol). CT_{\uparrow} is destabilized (arrow) and approaches TT , and the two are strongly mixed by the dihedral oscillation (color scale), resulting in coherent singlet fission. Exciting CT_{\uparrow} with more excess energy leads to superposition states with stronger TT contributions than within the thermally allowed region of CT_{\uparrow} (red dashed line). (c) Mixing between bright CT and TT as a function of solvent ϵ_r , at the fixed angle of $\Phi = 80^\circ$. Intermediate-polarity solvents result into maximal mixing and coherent singlet fission. This is compared with the experimental singlet fission rate, which we extract from the TT growth kinetics in SI Section S2.6. and the TT yields in Figure 5. The rate is optimized in solvents where singlet fission is coherent.

Here $J(\phi)$ and $\Lambda(\phi)$ are the couplings between states of the same symmetry along the symmetric torsional mode.

Due to the negligible Huang-Rhys factors of antisymmetric B modes compared to symmetric ones, their Franck-Condon factors and displacements are orders of magnitude smaller than those of A modes.^{70–72} Therefore, within our model approximation, we consider excess energy to only result in the displacement of A -symmetry modes, and to not generate any additional B symmetry vibrations. Since the singlet fission timescale in DT-Mes is relatively long (> 10 ps), we expect high-frequency A modes displaced via excess energy excitation to have mostly relaxed towards lower-frequency modes at these timescales. We further simplify the problem by approximating the resulting low-frequency mode distribution only in terms of motion along Φ . Consequently, within this model approach, excess-energy excitation leads to larger-amplitude oscillations along Φ , accessing higher regions of that surface. Importantly for this picture, the initial step of vibrational relaxation does not remove energy from the molecule but only redistributes it into other motions. These are damped through subsequent vibrational cooling, which for isolated molecules in solution is mediated by solvent-solute interactions,

e.g. collisions between DT-Mes and solvent molecules. This diffusion-mediated cooling can require many tens of ps.^{73–76} The excess vibrational energy in this ‘hot’ state manifested as large-amplitude Φ oscillations can thus persist on timescales relevant to singlet fission.

We now turn our attention to incorporating solvent effects into our description. In a polar solvent, local electric fields may be randomly oriented, leading to an energetic separation of the two CT states which inevitably appear in such a dimer molecule, with dipoles pointing in opposite directions. We refer to the stabilized and destabilized CT states as CT_{\downarrow} and CT_{\uparrow} . These states are symmetry-broken, as the solvent can generally arrange itself in a non-symmetric fashion around DT-Mes. This phenomenon is mathematically captured by introducing an additional coupling Δ between symmetry-pure CT_A and CT_B , which mixes them into the new eigenstates:

$$H_{el} = \begin{bmatrix} E_{LE_B}(\phi) & \eta & J(\phi) & 0 & 0 \\ \eta & E_{LE_A}(\phi) & 0 & 0 & 0 \\ J(\phi) & 0 & E_{CT_B}(\phi) & \eta + \Delta & 0 \\ 0 & 0 & \eta + \Delta & E_{CT_A}(\phi) & \Lambda(\phi) \\ 0 & 0 & 0 & \Lambda(\phi) & E_{TT}(\phi) \end{bmatrix}. \quad (4)$$

Physically, this expresses the fact that in the presence of an electric field it is the CT states with a permanent dipole and not the symmetry-adapted CT states which are eigenstates of the system.

We can determine the values of Δ corresponding to different solvent ϵ_r by benchmarking against the measured energetic stabilization CT_{\downarrow} (Figure 5b). For intermediate-polarity solvents, we find that CT_{\downarrow} and LE_B are energetically very close, leading to a strong mixing and transfer of oscillator strength from LE to CT, i.e. intensity borrowing.⁷⁷ This description closely reproduces the experimental trend of Figure 1c for the molar extinction coefficient, which is minimized in intermediate-polarity solvents. The calculated molar extinction coefficient is shown in SI Section S1.3 for a range of solvents. If the equivalently destabilized state CT_{\uparrow} were to form, we would in principle expect it to relax into CT_{\downarrow} . However, this process should occur through reorganization of the solvent shell and would be expected to occur on the few- to tens-picosecond timescale.⁷⁸ Accordingly, we would not expect to detect any photon emission from CT_{\uparrow} , since the relevant emission lifetime is tens of nanoseconds (for CT_{\downarrow} , SI Section S2.9). This timescale remains sufficiently long, though, for CT_{\uparrow} to play an important role in singlet fission despite being an unstable state.

Coherent and incoherent singlet fission. We can use this framework for the DT-Mes electronic structure to rationalize the surprising behavior in Figure 5. Our transient absorption experiments reveal TT is never formed directly from initial LE_B but is always preceded by CT states (Figure 3b and SI Section S2.6), and it only forms in conditions where CT is already formed with high efficiency (Figure 5a). The only major distinction between fission regimes occurs in the subsequent transition, from CT to TT, where the symmetry of the system must be broken. This step is the chief focus of our analysis, and we consider two limiting cases. In low-polarity solvents, $\eta > \Delta$ and vibronic effects provide the symmetry-breaking needed to access TT. In intermediate-polarity solvents, $\eta \ll \Delta$ and the symmetry-breaking is dominated by solvent effects. In either case, the CT states formed may initially be vibrationally ‘hot’ due to excess-energy excitation. Moreover, potentially either

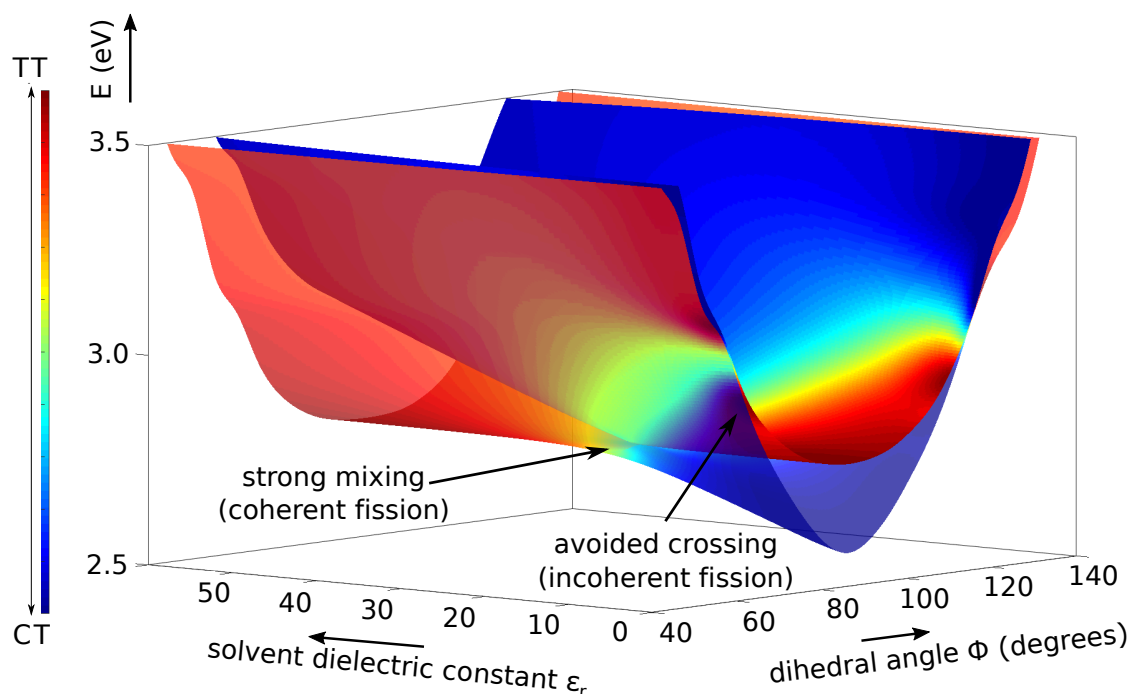


Figure 7 Adiabatic potential energy surfaces along the dihedral angle Φ and the solvent dielectric constant, showing their CT (blue) and TT (red) character. For low-polarity solvents the surfaces only mix for large-amplitude oscillations along Φ in the vicinity of an avoided crossing, leading to incoherent fission. Strong mixing is induced in intermediate-polarity solvents (e.g. ethanol), making singlet fission coherent. Finally, very polar solvents once again lead to reduced mixing between the surfaces.

CT_{\downarrow} or CT_{\uparrow} may be present, since both are mixed with CT_B and thus accessible from LE_B . A Marcus-like analysis of the CT_{\uparrow} to TT transition is discussed in SI section S1.4, along with its limitations.

The CT_{\uparrow} and TT potential energy surfaces along Φ for low-polarity solvents are given in Figure 6a, coded for their CT/TT character. In this case, CT_{\uparrow} and CT_{\downarrow} are almost degenerate. CT_{\uparrow} does not develop any TT character within the region accessible at room temperature (nor does CT_{\downarrow}), and the TT surface also remains pure. Within this model, a transition between the states is possible only through the avoided crossing that appears at larger angles, making singlet fission incoherent.^{9,18} Excitation of a hot state which can access that part of the potential energy landscape corresponds to an excess energy of about 0.4 eV. Excitation with still greater energy would not have a significant effect on the triplet yield, as the mixing is always negligible away from the crossing and no additional *B*-type (i.e. coupling) vibrations are generated. This is in close agreement with the experimental observation that a sharp threshold for TT formation appears at 0.33 eV of excess-energy excitation (Figure 5), with little dependence above that.

In intermediate-polarity solvents, the transient solvation dynamics which stabilize CT_{\downarrow} also destabilize CT_{\uparrow} to near the energy of TT. This results in a mixing of the two states through the dihedral rotation along Φ , as shown in Figure 6b. The contribution of each component varies along the potential energy surface, with the TT character (red shading) increasing away from the FC point. This is the regime of coherent singlet fission, as defined in previous studies.⁹ Hence exciting the system at higher energies leads to superposition states which are more ‘TT rich’, leading to stronger couplings to the final, relaxed TT state. A superposition of TT and CT_{\uparrow} eventually dephases towards its constituents, which are the relevant eigenstates of the system at its equilibrium

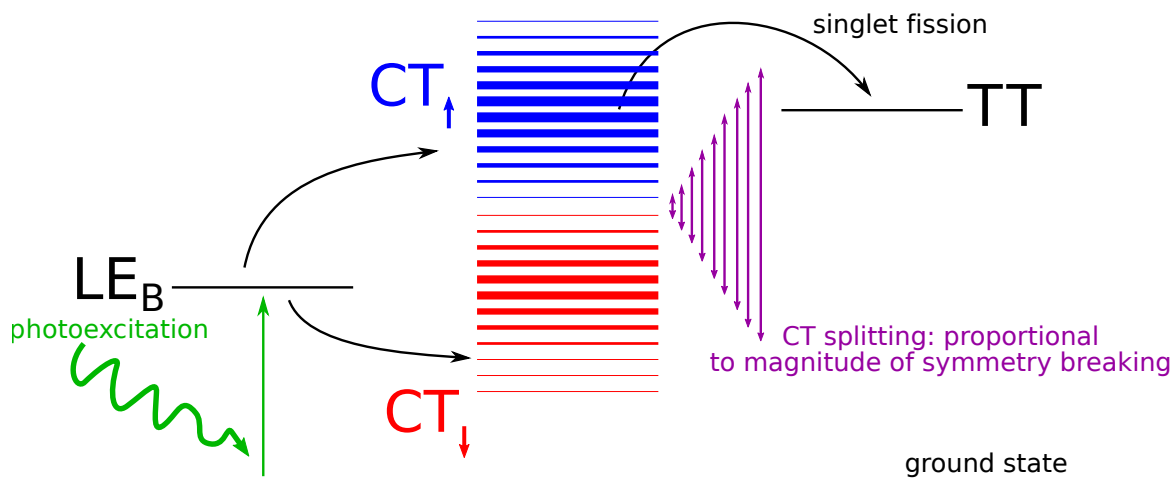


Figure 8 | Switching the singlet fission mechanism. Following photoexcitation to the bright LE_B state, the CT_{\uparrow} and CT_{\downarrow} states get populated. The thickness of these two states denotes their mixing with TT and LE_B respectively. Symmetry-breaking interactions (solvent effects in our study) control their splitting and consequently the mixing with the other electronic states. Coherent singlet fission takes place in the regime of high mixing between CT_{\uparrow} and TT .

geometry. The larger the TT contribution, the more likely it is that the system will collapse towards the final, relaxed TT state. In this regime the destabilized CT_{\uparrow} state is the ‘gateway’ for singlet fission regardless of excitation energy, and we would thus expect the TT yield to track the accessibility of CT_{\uparrow} . Experimentally, this would translate into the energy distribution inferred in Figure 5a (right), which is exactly what is observed. At the same time, regions of the surface with high TT contributions exhibit reduced CT character, leading to an anti-correlation of the TT and long-lived CT yields.

The increased degree of mixing between the CT and TT surfaces with increasing solvent polarity is reflected in the fission rates shown in Figure 6c, extracted from the TT growth kinetics in the transient absorption data in SI Section S2.6 and the TT yields in Figure 5a. Initially, increasing the solvent polarity increases the rate of singlet fission, but in very polar solvents the TT formation rate drops again to low values. In these solvents CT_{\uparrow} shifts above the TT surface and the two stop mixing, leading to a regime of incoherent fission similar to the non-polar case. This mixing is quantified via $\rho_{CT_B TT}$ of Equation 2, which we plot in Figure 6c for the fixed angle $\Phi = 80^\circ$ as a function of solvent dielectric constant. Note that this is calculated in the original basis of symmetry-pure CT states which form CT_{\uparrow} . In summary, we find that intermediate-polarity solvents lead to maximal mixing between CT_B and TT , thus leading to coherent singlet fission. In this case, TT is formed via the dephasing of the CT_{\uparrow}/TT superposition, which is more efficient and has qualitative differences compared to incoherent TT formation through an avoided crossing. Hence intermediate polarity solvents provide an optimal regime for singlet fission, qualitatively reproducing the experimental trend for the singlet fission rates. The different singlet fission regimes are summarized in the multidimensional plot of Figure 7 for the CT_{\uparrow} and TT surfaces. For the different dihedral angles and solvent dielectric constants, the surfaces are annotated with the respective CT/TT contribution as a color code.

Conclusions

Our results demonstrate not only that intramolecular singlet fission in DT-Mes is a ‘hot’ process mediated by an

1
2
3 unusual ‘destabilized’ CT state, but also that the system can explore coherent and incoherent regimes of singlet
4 fission. This is achieved by exploiting symmetry-breaking solvent interactions to induce the necessary energetic
5 proximity for a vibrational mode to mix the CT and TT states. Interestingly, these interactions are by their
6 nature transient, driven by changes in the solvation shell. Here, the precise degree of mixing depends on the
7 solvent polarity, allowing us to switch between coherent and incoherent fission in different solvents and explore
8 the effects in detail through altering the energy of excitation. In addition, while coherent singlet fission has been
9 reported to occur due to mixing between the bright singlet and TT states,^{6,7,9,18} it is to our knowledge the
10 first time that the role of CT/TT mixing for coherent fission is studied in detail. The fact that singlet fission in
11 DT-Mes occurs through a real CT intermediate underlines the importance of this second step of fission and the
12 advantages of a system dependent on CT states, which are markedly easier to control through environmental
13 factors such as solvent polarity than LE states.
14
15

16
17
18
19 Our approach for controlling the fission mechanism also indicates a more general concept, where various
20 symmetry-breaking effects could be used as ‘switches’ between coherent and incoherent regimes. External
21 electric fields and strong coupling to light⁷⁹ could potentially provide a similar symmetry-breaking effect on the
22 CT states, leading to a coherent fission regime in the vicinity of large mixing, as visualized in Figure 8. The
23 same could be achieved through chemical synthesis, or through changes in the crystal symmetry. Experiments¹⁰
24 and calculations⁸⁰ indicate that the rate of fission closely depends on the crystal structure. Tetracene and TIPS-
25 tetracene exhibit strikingly different fission properties for highly crystalline versus symmetry-broken amorphous
26 or polycrystalline films,^{10,16,81} indicating a possible transition between coherent and incoherent fission within
27 the same material. Singlet fission is but one example of a photophysical process where the efficiency may be
28 tuned by entering a coherent regime. The same underlying principle could also be used to manipulate and
29 ultimately enhance processes as diverse as long-range energy transport, biomimetic light harvesting and charge
30 separation at interfaces in solar cells.^{82,83}
31
32
33
34
35
36
37
38

39 Methods

40 Computations

41
42
43 In order to obtain the energies of the ground state at the different dihedral angles Φ , constrained geometry optimizations along
44 Φ were performed using density functional theory (DFT), employing the cc-pVDZ basis set and the B3LYP functional. The
45 DFT calculations allow us to take steric effects into account. To accurately account for conjugation effects on the excited states,
46 excited state calculations at all geometries were performed by using the Pople-Parr-Pariser (PPP) theory. Details on the used PPP
47 parameters and the rest of the computational methodology are given in SI Section S1. The results on the electronic structure and
48 geometries are used to define a model Hamiltonian as outlined in SI Section S1.2. This includes the effect of the dihedral rotation
49 on the electronic structure, as well as that of the solvent through the control parameter Δ . By diagonalizing the Hamiltonian at
50 different dihedral angles, we obtain the wavefunctions and energies of the system.
51
52
53
54
55
56
57
58
59
60

Acknowledgements

This work was supported by the Engineering and Physical Sciences Research Council, UK (grant numbers EP/L015552/1, EP/M025330/1 and EP/M005143/1). A.M.A. acknowledges the support of the Winton Programme for the Physics of Sustainability. S.L. thanks A*STAR Graduate Scholarship support from A*STAR Singapore. T.J.H.H. acknowledges a Research Fellowship from Jesus College, Cambridge. E.G.F. acknowledges financial support from the National Science Foundation Award No. CHE-1555205. J. W. acknowledges financial support from the MOE Tier 3 programme (MOE2014-T3-1-004). The authors thank Akshay Rao for useful discussions and for commenting on the manuscript.

Data Availability

The data underlying this publication is available at [URL added in proof].

Additional Information

Supporting Information. Details on the computational methodology, synthesis, and experimental setup and procedure can be found at [URL added in proof].

Competing interests: The authors declare no competing interests

References

- ¹ Millicent B. Smith and Josef Michl. Singlet fission. *Chemical Reviews*, 110(11):6891–6936, 2010.
- ² M. C. Hanna and A. J. Nozik. Solar conversion efficiency of photovoltaic and photoelectrolysis cells with carrier multiplication absorbers. *Journal of Applied Physics*, 100(7), 2006.
- ³ Akshay Rao and Richard H Friend. Harnessing singlet exciton fission to break the Shockley–Queisser limit. *Nature Reviews Materials*, 2:17063, oct 2017.
- ⁴ DN Congreve, Jiye Lee, NJ Thompson, and Eric Hontz. External Quantum Efficiency Above 100% in a Singlet-Exciton-Fission-Based Organic Photovoltaic Cell. *Science*, 340(6130):334–337, 2013.
- ⁵ Wai Lun Chan, Manuel Ligges, Askat E. Jailaubekov, Loren G. Kaake, Luis Miaja-Avila, and X.-Y. Zhu. Observing the Multiexciton State in Singlet Fission and Ensuing Ultrafast Multielectron Transfer. *Science*, 334(December):1541–1545, 2011.
- ⁶ Wai Lun Chan, Timothy C. Berkelbach, Makenzie R. Provorse, Nicholas R. Monahan, John R. Tritsch, Mark S. Hybertsen, David R. Reichman, Jiali Gao, and X. Y. Zhu. The quantum coherent mechanism for singlet fission: Experiment and theory. *Accounts of Chemical Research*, 46(6):1321–1329, 2013.
- ⁷ Eric C. Greyson, Josh Vura-Weis, Josef Michl, and Mark A. Ratner. Maximizing singlet fission in organic dimers: Theoretical investigation of triplet yield in the regime of localized excitation and fast coherent electron transfer. *Journal of Physical Chemistry B*, 114(45):14168–14177, 2010.
- ⁸ Nicholas R. Monahan, Dezheng Sun, Hiroyuki Tamura, Kristopher W. Williams, Bolei Xu, Yu Zhong, Bharat Kumar, Colin Nuckolls, Avetik R. Harutyunyan, Gugang Chen, Hai Lung Dai, David Beljonne, Yi Rao, and X. Y. Zhu. Dynamics of the triplet-pair state reveals the likely coexistence of coherent and incoherent singlet fission in crystalline hexacene. *Nature Chemistry*, 9(4):341–346, 2017.
- ⁹ Kiyoshi Miyata, Yuki Kurashige, Kazuya Watanabe, Toshiki Sugimoto, Shota Takahashi, Shunsuke Tanaka, Jun Takeya, Takeshi Yanai, and Yoshiyasu Matsumoto. Coherent singlet fission activated by symmetry breaking. *Nature Chemistry*, 9(10):983–989, 2017.

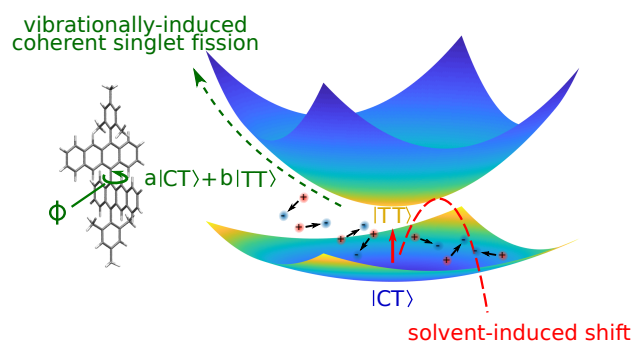
- 1
2
3
4
5
6
7
8
9
10
11
12
13
14
15
16
17
18
19
20
21
22
23
24
25
26
27
28
29
30
31
32
33
34
35
36
37
38
39
40
41
42
43
44
45
46
47
48
49
50
51
52
53
54
55
56
57
58
59
60
- ¹⁰ Shane R Yost, Jiye Lee, Mark W B Wilson, Tony Wu, David P McMahon, Rebecca R Parkhurst, Nicholas J Thompson, Daniel N Congreve, Akshay Rao, Kerr Johnson, Matthew Y Sfeir, Mounqi G Bawendi, Timothy M Swager, Richard H Friend, Marc a Baldo, and Troy Van Voorhis. A transferable model for singlet-fission kinetics. *Nature Chemistry*, 6(6):492–497, 2014.
- ¹¹ Paul M Zimmerman, Zhiyong Zhang, and Charles B Musgrave. Singlet fission in pentacene through multi-exciton quantum states. *Nature chemistry*, 2(8):648–652, 2010.
- ¹² C. E. Swenberg and W. T. Stacy. Bimolecular radiationless transitions in crystalline tetracene. *Chemical Physics Letters*, 2(5):327–328, 1968.
- ¹³ Jonathan J. Burdett and Christopher J. Bardeen. Quantum beats in crystalline tetracene delayed fluorescence due to triplet pair coherences produced by direct singlet fission. *Journal of the American Chemical Society*, 134(20):8597–8607, 2012.
- ¹⁴ Mark W.B. Wilson, Akshay Rao, Kerr Johnson, Simon G elinas, Riccardo Di Pietro, Jenny Clark, and Richard H. Friend. Temperature-independent singlet exciton fission in tetracene. *Journal of the American Chemical Society*, 135(44):16680–16688, 2013.
- ¹⁵ Murad J.Y. Tayebjee, Rapha el G.C.R. Clady, and Timothy W. Schmidt. The exciton dynamics in tetracene thin films. *Physical Chemistry Chemical Physics*, 15(35):14797–14805, 2013.
- ¹⁶ Hannah L. Stern, Alexandre Cheminal, Shane R. Yost, Katharina Broch, Sam L. Bayliss, Kai Chen, Maxim Tabachnyk, Karl Thorley, Neil Greenham, Justin M. Hodgkiss, John Anthony, Martin Head-Gordon, Andrew J. Musser, Akshay Rao, and Richard H. Friend. Vibronically coherent ultrafast triplet-pair formation and subsequent thermally activated dissociation control efficient endothermic singlet fission. *Nature Chemistry*, 9(12):1205–1212, 2017.
- ¹⁷ Jonathan J. Burdett, David Gosztola, and Christopher J. Bardeen. The dependence of singlet exciton relaxation on excitation density and temperature in polycrystalline tetracene thin films: Kinetic evidence for a dark intermediate state and implications for singlet fission. *Journal of Chemical Physics*, 135(21), 2011.
- ¹⁸ Wai Lun Chan, Manuel Ligges, and X. Y. Zhu. The energy barrier in singlet fission can be overcome through coherent coupling and entropic gain. *Nature Chemistry*, 4(10):840–845, 2012.
- ¹⁹ Andrew J Musser, Matz Liebel, Christoph Schnedermann, Torsten Wende, Tom B Kehoe, Akshay Rao, and Philipp Kukura. Evidence for conical intersection dynamics mediating ultrafast singlet exciton fission. *Nature Physics*, 11:352, mar 2015.
- ²⁰ Artem A. Bakulin, Sarah E. Morgan, Tom B. Kehoe, Mark W.B. Wilson, Alex W. Chin, Donatas Zigmantas, Dassia Egorova, and Akshay Rao. Real-time observation of multiexcitonic states in ultrafast singlet fission using coherent 2D electronic spectroscopy. *Nature Chemistry*, 8(1):16–23, 2016.
- ²¹ Roel Tempelaar and David R. Reichman. Vibronic exciton theory of singlet fission. III. How vibronic coupling and thermodynamics promote rapid triplet generation in pentacene crystals. *Journal of Chemical Physics*, 148(24), 2018.
- ²² Yuta Fujihashi, Lipeng Chen, Akihito Ishizaki, Junling Wang, and Yang Zhao. Effect of high-frequency modes on singlet fission dynamics. *Journal of Chemical Physics*, 146(4), 2017.
- ²³ Hiroyuki Tamura, Miquel Huix-Rotllant, Irene Burghardt, Yoann Olivier, and David Beljonne. First-Principles Quantum Dynamics of Singlet Fission: Coherent versus Thermally Activated Mechanisms Governed by Molecular π Stacking. *Physical Review Letters*, 115(10):1–5, 2015.
- ²⁴ Xintian Feng and Anna I. Krylov. On couplings and excimers: lessons from studies of singlet fission in covalently linked tetracene dimers. *Physical Chemistry Chemical Physics*, 18(11):7751–7761, 2016.
- ²⁵ Zhongkai Huang, Yuta Fujihashi, and Yang Zhao. Effect of Off-Diagonal Exciton-Phonon Coupling on Intramolecular Singlet Fission. *The Journal of Physical Chemistry Letters*, 8(14):3306–3312, jul 2017.
- ²⁶ Florian A. Y. N. Schr oder, David H. P. Turban, Andrew J. Musser, Nicholas D. M. Hine, and Alex W. Chin. Tensor network simulation of multi-environmental open quantum dynamics via machine learning and entanglement renormalisation. *Nature Communications*, 10(1):1062, 2019.

- 1
2
3 27 Steven Lukman, Kai Chen, Justin M. Hodgkiss, David H. P. Turban, Nicholas D. M. Hine, Shaoqiang Dong, Jishan Wu, Neil C.
4 Greenham, and Andrew J. Musser. Tuning the role of charge-transfer states in intramolecular singlet exciton fission through
5 side-group engineering. *Nature Communications*, 7:13622, 2016.
- 6
7 28 Eric G. Fuemmeler, Samuel N. Sanders, Andrew B. Pun, Elango Kumarasamy, Tao Zeng, Kiyoshi Miyata, Michael L. Steigerwald,
8 X. Y. Zhu, Matthew Y. Sfeir, Luis M. Campos, and Nandini Ananth. A direct mechanism of ultrafast intramolecular singlet
9 fission in pentacene dimers. *ACS Central Science*, 2(5):316–324, 2016.
- 10
11 29 Timothy C. Berkelbach, Mark S. Hybertsen, and David R. Reichman. Microscopic theory of singlet exciton fission. II. Application
12 to pentacene dimers and the role of superexchange. *Journal of Chemical Physics*, 138(11):114103, 2013.
- 13
14 30 Paul M. Zimmerman, Franziska Bell, David Casanova, and Martin Head-Gordon. Mechanism for singlet fission in pentacene and
15 tetracene: From single exciton to two triplets. *Journal of the American Chemical Society*, 133(49):19944–19952, 2011.
- 16
17 31 Millicent B. Smith and Josef Michl. Recent Advances in Singlet Fission. *Annual Review of Physical Chemistry*, 64(1):361–386,
18 2013.
- 19
20 32 Timothy C. Berkelbach, Mark S. Hybertsen, and David R. Reichman. Microscopic theory of singlet exciton fission. I. General
21 formulation. *The Journal of Chemical Physics*, 138(11):114102, 2013.
- 22
23 33 K. C. Krishnapriya, Palas Roy, Boregowda Puttaraju, Ulrike Salzner, Andrew J. Musser, Manish Jain, Jyotishman Dasgupta,
24 and Satish Patil. Spin density encodes intramolecular singlet exciton fission in pentacene dimers. *Nature Communications*, 10(1),
25 2019.
- 26
27 34 Samuel N. Sanders, Elango Kumarasamy, Andrew B. Pun, M. Tuan Trinh, Bonnie Choi, Jianlong Xia, Elliot J. Taffet, Jonathan Z.
28 Low, John R. Miller, Xavier Roy, X. Y. Zhu, Michael L. Steigerwald, Matthew Y. Sfeir, and Luis M. Campos. Quantitative
29 Intramolecular Singlet Fission in Bipentacenes. *Journal of the American Chemical Society*, 137(28):8965–8972, 2015.
- 30
31 35 Johannes Zirzmeier, Dan Lehnher, Pedro B. Coto, Erin T. Chernick, Rubén Casillas, Bettina S. Basel, Michael Thoss,
32 Rik R. Tykwinski, and Dirk M. Guldi. Singlet fission in pentacene dimers. *Proceedings of the National Academy of Sciences*,
33 112(17):5325–5330, 2015.
- 34
35 36 Nadezhda V. Korovina, Saptaparna Das, Zachary Nett, Xintian Feng, Jimmy Joy, Ralf Haiges, Anna I. Krylov, Stephen E.
36 Bradforth, and Mark E. Thompson. Singlet Fission in a Covalently Linked Cofacial Alkynyltetracene Dimer. *Journal of the*
37 *American Chemical Society*, 138(2):617–627, 2016.
- 38
39 37 Justin C. Johnson, Arthur J. Nozik, and Josef Michl. The role of chromophore coupling in singlet fission. *Accounts of Chemical*
40 *Research*, 46(6):1290–1299, 2013.
- 41
42 38 Elango Kumarasamy, Samuel N. Sanders, Murad J.Y. Tayebjee, Amir Asadpoordarvish, Timothy J.H. Hele, Eric G. Fuemmeler,
43 Andrew B. Pun, Lauren M. Yablon, Jonathan Z. Low, Daniel W. Paley, Jacob C. Dean, Bonnie Choi, Gregory D. Scholes,
44 Michael L. Steigerwald, Nandini Ananth, Dane R. McCamey, Matthew Y. Sfeir, and Luis M. Campos. Tuning Singlet Fission in
45 π -Bridge- π Chromophores. *Journal of the American Chemical Society*, 139(36):12488–12494, 2017.
- 46
47 39 Bettina S Basel, Johannes Zirzmeier, Constantin Hetzer, Brian T Phelan, Matthew D Krzyaniak, S Rajagopala Reddy, Pedro B
48 Coto, Noah E Horwitz, Ryan M Young, Fraser J White, Frank Hampel, Timothy Clark, Michael Thoss, Rik R Tykwinski,
49 Michael R Wasielewski, and Dirk M Guldi. Unified model for singlet fission within a non-conjugated covalent pentacene dimer.
50 *Nature Communications*, 8(May):15171, may 2017.
- 51
52 40 Jasper D Cook, Thomas James Carey, Dylan H. Arias, Justin C. Johnson, and Niels H. Damrauer. Solvent-Controlled Branching
53 of Localized versus Delocalized Singlet Exciton States and Equilibration with Charge Transfer in a Structurally Well-Defined
54 Tetracene Dimer. *The Journal of Physical Chemistry A*, 121(48):9229–9242, dec 2017.
- 55
56 41 Nadezhda V. Korovina, Jimmy Joy, Xintian Feng, Cassidy Feltenberger, Anna I. Krylov, Stephen E. Bradforth, and Mark E.
57 Thompson. Linker-Dependent Singlet Fission in Tetracene Dimers. *Journal of the American Chemical Society*, 140(32):10179–
58 10190, 2018.

- 1
2
3 42 Takuya Yamakado, Shota Takahashi, Kazuya Watanabe, Yoshiyasu Matsumoto, Atsuhiko Osuka, and Shohei Saito. Conformational Planarization versus Singlet Fission: Distinct Excited-State Dynamics of Cyclooctatetraene-Fused Acene Dimers. *Angewandte Chemie International Edition*, 57(19):5438–5443, may 2018.
- 4
5
6
7 43 Takao Sakuma, Hayato Sakai, Yasuyuki Araki, Tadashi Mori, Takehiko Wada, Nikolai V. Tkachenko, and Taku Hasobe. Long-Lived Triplet Excited States of Bent-Shaped Pentacene Dimers by Intramolecular Singlet Fission. *Journal of Physical Chemistry A*, 120(11):1867–1875, 2016.
- 8
9
10
11 44 Steven Lukman, Andrew J. Musser, Kai Chen, Stavros Athanasopoulos, Chaw K. Yong, Zebing Zeng, Qun Ye, Chunyan Chi, Justin M. Hodgkiss, Jishan Wu, Richard H. Friend, and Neil C. Greenham. Tuneable Singlet Exciton Fission and Triplet-Triplet Annihilation in an Orthogonal Pentacene Dimer. *Advanced Functional Materials*, 25(34):5452–5461, 2015.
- 12
13
14
15 45 Eric A. Margulies, Claire E. Miller, Yilei Wu, Lin Ma, George C. Schatz, Ryan M. Young, and Michael R. Wasielewski. Enabling singlet fission by controlling intramolecular charge transfer in π -stacked covalent terrylenediimide dimers. *Nature Chemistry*, 8(12):1120–1125, 2016.
- 16
17
18
19 46 Andrew J. Musser, Mohammed Al-Hashimi, Margherita Maiuri, Daniele Brida, Martin Heeney, Giulio Cerullo, Richard H. Friend, and Jenny Clark. Activated singlet exciton fission in a semiconducting polymer. *Journal of the American Chemical Society*, 135(34):12747–12754, 2013.
- 20
21
22
23 47 Karsten Elich, Minoru Kitazawa, Tadashi Okada, and Rüdiger Wortmann. Effect of S₁ Torsional Dynamics on the Time-Resolved Fluorescence Spectra of 9,9'-Bianthryl in Solution. *The Journal of Physical Chemistry A*, 101(96):2010–2015, 1997.
- 24
25
26
27 48 Yuxiang Mo, Jiangtao Lei, Yunxiang Sun, Qingwen Zhang, and Guanghong Wei. Conformational Ensemble of hIAPP Dimer: Insight into the Molecular Mechanism by which a Green Tea Extract inhibits hIAPP Aggregation. *Scientific Reports*, 6(May):1–11, 2016.
- 28
29
30
31 49 C. A. Coulson and G. S. Rushbrooke. Note on the method of molecular orbitals. *Mathematical Proceedings of the Cambridge Philosophical Society*, 36(2):193–200, 1940.
- 32
33
34
35 50 N. J. Hestand, H. Yamagata, Bolei Xu, Dezheng Sun, Yu Zhong, Avetik R. Harutyunyan, Gugang Chen, Hai Lung Dai, Yi Rao, and F. C. Spano. Polarized absorption in crystalline pentacene: Theory vs experiment. *Journal of Physical Chemistry C*, 119(38):22137–22147, 2015.
- 36
37
38
39 51 G. Wilse Robinson. Intensity enhancement of forbidden electronic transitions by weak intermolecular interactions. *The Journal of Chemical Physics*, 46(2):572–585, 1967.
- 40
41
42
43 52 Annamaria Petrozza, Frédéric Laquai, Ian A. Howard, Ji-Seon Kim, and Richard H. Friend. Dielectric switching of the nature of excited singlet state in a donor-acceptor-type polyfluorene copolymer. *Phys. Rev. B*, 81:205421, May 2010.
- 44
45
46
47 53 Shunichi Fukuzumi, Hiroaki Kotani, Kei Ohkubo, Seiji Ogo, Nikolai V. Tkachenko, and Helge Lemmetyinen. Electron-Transfer State of 9-Mesityl-10-methylacridinium Ion with a Much Longer Lifetime and Higher Energy Than That of the Natural Photosynthetic Reaction Center. *Journal of the American Chemical Society*, 126(6):1600–1601, 2004.
- 48
49
50
51 54 Samuel W. Eaton, Leah E. Shoer, Steven D. Karlen, Scott M. Dyar, Eric A. Margulies, Brad S. Veldkamp, Charusheela Ramanan, Daniel A. Hartzler, Sergei Savikhin, Tobin J. Marks, and Michael R. Wasielewski. Singlet exciton fission in polycrystalline thin films of a slip-stacked perylenediimide. *Journal of the American Chemical Society*, 135(39):14701–14712, 2013.
- 52
53
54
55 55 Hannah L. Stern, Andrew J. Musser, Simon Gelin, Patrick Parkinson, Laura M. Herz, Matthew J. Bruzek, John Anthony, Richard H. Friend, and Brian J. Walker. Identification of a triplet pair intermediate in singlet exciton fission in solution. *Proceedings of the National Academy of Sciences*, 112(25):7656–7661, 2015.
- 56
57
58
59 56 Hiroki Nagashima, Shuhei Kawaoka, Seiji Akimoto, Takashi Tachikawa, Yasunori Matsui, Hiroshi Ikeda, and Yasuhiro Kobori. Singlet-Fission-Born Quintet State: Sublevel Selections and Trapping by Multiexciton Thermodynamics. *Journal of Physical Chemistry Letters*, 9(19):5855–5861, 2018.
- 60
57 Kai Chen, Joseph K. Gallaher, Alex J. Barker, and Justin M. Hodgkiss. Transient grating photoluminescence spectroscopy: An ultrafast method of gating broadband spectra. *Journal of Physical Chemistry Letters*, 5(10):1732–1737, 2014.

- 1
2
3 58 Martin Jurczok, Pascal Plaza, Monique M. Martin, Yves H. Meyer, and Wolfgang Rettig. Excited state relaxation paths in
4 9,9'-bianthryl and 9-carbazoyl-anthracene: A sub-ps transient absorption study. *Chemical Physics*, 253(2-3):339–349, 2000.
- 5 59 C. Burgdorff, T. Kircher, and H. G. Löhmannsröben. Photophysical properties of tetracene derivatives in solution. *Spectrochimica*
6 *Acta Part A: Molecular Spectroscopy*, 44(11):1137–1141, 1988.
- 7
8 60 Akshay Rao, Philip C Y Chow, Simon Gélinas, Cody W Schlenker, Chang-Zhi Li, Hin-Lap Yip, Alex K-Y Jen, David S Ginger,
9 and Richard H Friend. The role of spin in the kinetic control of recombination in organic photovoltaics. *Nature*, 500(7463):435–9,
10 2013.
- 11
12 61 Samuel N. Sanders, Elango Kumarasamy, Andrew B. Pun, Michael L. Steigerwald, Matthew Y. Sfeir, and Luis M. Campos.
13 Intramolecular Singlet Fission in Oligoacene Heterodimers. *Angewandte Chemie - International Edition*, 55(10):3373–3377,
14 2016.
- 15
16 62 Murad J.Y. Tayebjee, Samuel N. Sanders, Elango Kumarasamy, Luis M. Campos, Matthew Y. Sfeir, and Dane R. McCamey.
17 Quintet multiexciton dynamics in singlet fission. *Nature Physics*, 13(2):182–188, 2017.
- 18
19 63 Erik Busby, Jianlong Xia, Qin Wu, Jonathan Z. Low, Rui Song, John R. Miller, X. Y. Zhu, Luis M. Campos, and Matthew Y.
20 Sfeir. A design strategy for intramolecular singlet fission mediated by charge-transfer states in donor-acceptor organic materials.
21 *Nature Materials*, 14(4):426–433, 2015.
- 22
23 64 Yukitomo Kasai, Yasunari Tamai, Hideo Ohkita, Hiroaki Bente, and Shinzaburo Ito. Ultrafast Singlet Fission in a Push-Pull
24 Low-Bandgap Polymer Film. *Journal of the American Chemical Society*, 137(51):15980–15983, 2015.
- 25
26 65 Anatoly B. Kolomeisky, Xintian Feng, and Anna I. Krylov. A simple kinetic model for singlet fission: A role of electronic and
27 entropic contributions to macroscopic rates. *Journal of Physical Chemistry C*, 118(10):5188–5195, 2014.
- 28
29 66 Chaw Keong Yong, Andrew J. Musser, Sam L. Bayliss, Steven Lukman, Hiroyuki Tamura, Olga Bubnova, Rawad K. Hallani,
30 Aurelie Meneau, Roland Resel, Munetaka Maruyama, Shu Hotta, Laura M. Herz, David Beljonne, John E. Anthony, Jenny
31 Clark, and Henning Sirringhaus. The entangled triplet pair state in acene and heteroacene materials. *Nature Communications*,
32 8(May):15953, 2017.
- 33
34 67 Steven Lukman, Johannes M. Richter, Le Yang, Pan Hu, Jishan Wu, Neil C. Greenham, and Andrew J. Musser. Efficient
35 Singlet Fission and Triplet-Pair Emission in a Family of Zethrene Diradicaloids. *Journal of the American Chemical Society*,
36 139(50):18376–18385, 2017.
- 37
38 68 Andrew J. Musser and Jenny Clark. Triplet-pair states in organic semiconductors. *Annual Review of Physical Chemistry*,
39 70:323–351, 2019.
- 40
41 69 Xintian Feng, Anatoliy V. Luzanov, and Anna I. Krylov. Fission of entangled Spins: An electronic structure perspective. *Journal*
42 *of Physical Chemistry Letters*, 4(22):3845–3852, 2013.
- 43
44 70 Clark Robin J H and Trevor J Dines. Resonance Raman Spectroscopy, and Its Application to Inorganic Chemistry. *Angewandte*
45 *Chemie - International Edition*, 25:131–158, 1986.
- 46
47 71 H. Köppel, Wolfgang Domcke, and Lorenz S Cederbaum. *Advances in Chemical Physics, Volume 57, Multimode Molecular*
48 *Dynamics Beyond the Born-Oppenheimer Approximation*, pages 102–110. 1984.
- 49
50 72 Fabrizia Negri and G. Orlandi. *Computational Photochemistry, Chapter IV*, pages 129–139. Elsevier, 2005.
- 51
52 73 Xin Tan, Terry L. Gustafson, Christophe Lefumeux, Gotard Burdzinski, Guy Buntinx, and Olivier Poizat. Solvation dynamics
53 probed by femtosecond transient absorption spectroscopy: Vibrational cooling and conformational relaxation in S1 trans-4,4-
54 diphenylstilbene. *Journal of Physical Chemistry A*, 106(14):3593–3598, 2002.
- 55
56 74 A. Weigel and N. P. Ernstring. Excited Stilbene: Intramolecular Vibrational Redistribution and Solvation Studied by Femtosecond
57 Stimulated Raman Spectroscopy. *Journal of Physical Chemistry B*, 114(23):7879–7893, 2010.
- 58
59 75 Michael P. Grubb, Philip M. Coulter, Hugo J.B. Marroux, Balazs Hornung, Ryan S. McMullen, Andrew J. Orr-Ewing, and
60 Michael N.R. Ashfold. Translational, rotational and vibrational relaxation dynamics of a solute molecule in a non-interacting
solvent. *Nature Chemistry*, 8(11):1042–1046, 2016.

- 1
2
3 ⁷⁶ Michael P. Grubb, Philip M. Coulter, Hugo J.B. Marroux, Andrew J. Orr-Ewing, and Michael N.R. Ashfold. Unravelling the
4 mechanisms of vibrational relaxation in solution. *Chemical Science*, 8(4):3062–3069, 2017.
- 5
6 ⁷⁷ Timothy John Harvey Hele, Eric G Fuemmeler, Samuel N Sanders, Elango Kumarasamy, Matthew Y. Sfeir, Luis M. Campos, and
7 Nandini Ananth. Anticipating Acene-based Chromophore Spectra with Molecular Orbital Arguments. *The Journal of Physical*
8 *Chemistry A*, 123:2527–2536, 2019.
- 9
10 ⁷⁸ W. M. Kwok, C. Ma, M. W. George, D. C. Grills, P. Matousek, A. W. Parker, D. Phillips, W. T. Toner, and M. Towrie.
11 Solvent effects on the charge transfer excited states of 4-dimethylaminobenzonitrile (DMABN) and 4-dimethylamino-3,5-
12 dimethylbenzonitrile (TMABN) studied by time-resolved infrared spectroscopy: a direct observation of hydrogen bonding inter-
13 actions. *Photochemical & Photobiological Sciences*, 6(9):987, 2007.
- 14
15 ⁷⁹ Daniel Polak, Rahul Jayaprakash, Anastasia Leventis, Kealan J Fallon, Harriet Coulthard, Anthony J. Petty, John Anthony,
16 Hugo Bronstein, David G Lidzey, Jenny Clark, and Andrew J Musser. Manipulating matter with strong coupling: harvesting
17 triplet excitons in organic exciton microcavities. *arXiv*, page 1806.09990, 2018.
- 18
19 ⁸⁰ Sivan Refaely-Abramson, Felipe H. Da Jornada, Steven G. Louie, and Jeffrey B. Neaton. Origins of Singlet Fission in Solid
20 Pentacene from an ab initio Green's Function Approach. *Physical Review Letters*, 119(26):1–6, 2017.
- 21
22 ⁸¹ Geoffrey B. Piland and Christopher J. Bardeen. How Morphology Affects Singlet Fission in Crystalline Tetracene. *Journal of*
23 *Physical Chemistry Letters*, 6(10):1841–1846, 2015.
- 24
25 ⁸² Simon Gélinas, Akshay Rao, Abhishek Kumar, Samuel L Smith, Alex W Chin, Jenny Clark, Tom S van der Poll, Guillermo C
26 Bazan, and Richard H Friend. Ultrafast long-range charge separation in organic semiconductor photovoltaic diodes. *Science*
27 *(New York, N.Y.)*, 343(6170):512–6, 2014.
- 28
29 ⁸³ Gregory D. Scholes, Graham R. Fleming, Lin X. Chen, Alán Aspuru-Guzik, Andreas Buchleitner, David F. Coker, Gregory S.
30 Engel, Rienk Van Grondelle, Akihito Ishizaki, David M. Jonas, Jeff S. Lundeen, James K. McCusker, Shaul Mukamel, Jennifer P.
31 Ogilvie, Alexandra Olaya-Castro, Mark A. Ratner, Frank C. Spano, K. Birgitta Whaley, and Xiaoyang Zhu. Using coherence to
32 enhance function in chemical and biophysical systems. *Nature*, 543(7647):647–656, 2017.
- 33
34
35
36
37
38
39
40
41
42
43
44
45
46
47
48
49
50
51
52
53
54
55
56
57
58
59
60



For Table of Contents Only